

## 13.2. Rotation functions

BY J. NAVAZA

### 13.2.1. Overview

We will discuss a technique to find either the relative orientations of homologous but independent subunits connected by noncrystallographic symmetry (NCS) elements or the absolute orientations of these subunits if the structure of a similar molecule or fragment is available. The procedure makes intensive use of properties of the rotation group, so we will start by recalling some properties of rotations. More advanced results are included in Appendix 13.2.1.

### 13.2.2. Rotations in three-dimensional Euclidean space

A rotation  $\mathbf{R}$  is specified by an oriented axis, characterized by the unit vector  $\mathbf{u}$ , and the spin,  $\chi$ , about it. Positive spins are defined by the right-hand screw sense and values are given in degrees. An almost one-to-one correspondence between rotations and parameters  $(\chi, \mathbf{u})$  can be established. If we restrict the spin values to the positive interval  $0 \leq \chi \leq 180$ , then for each rotation there is a unique vector  $\chi\mathbf{u}$  within the sphere of radius 180. However, vectors situated at opposite points on the surface correspond to the same rotation, e.g.  $(180, \mathbf{u})$  and  $(180, -\mathbf{u})$ .

When the unit vector  $\mathbf{u}$  is specified by the colatitude  $\omega$  and the longitude  $\varphi$  with respect to an orthonormal reference frame (see Fig. 13.2.2.1a), we have the spherical polar parameterization of rotations  $(\chi, \omega, \varphi)$ . The range of variation of the parameters is

$$0 \leq \chi \leq 180; 0 \leq \omega \leq 180; 0 \leq \varphi < 360.$$

Rotations may also be parameterized with the Euler angles  $(\alpha, \beta, \gamma)$  associated with an orthonormal frame  $(\mathbf{x}, \mathbf{y}, \mathbf{z})$ . Several conventions exist for the names of angles and definitions of the axes involved in this parameterization. We will follow the convention by which  $(\alpha, \beta, \gamma)$  denotes a rotation of  $\alpha$  about the  $z$  axis, followed by a rotation of  $\beta$  about the nodal line  $n$ , the rotated  $y$  axis, and finally a rotation of  $\gamma$  about  $\mathbf{p}$ , the rotated  $z$  axis (see Fig. 13.2.2.1b):

$$\mathbf{R}(\alpha, \beta, \gamma) = \mathbf{R}(\gamma, \mathbf{p})\mathbf{R}(\beta, \mathbf{n})\mathbf{R}(\alpha, \mathbf{z}). \quad (13.2.2.1)$$

The same rotation may be written in terms of rotations around the fixed orthonormal axes. By using the group property

$$\mathbf{TR}(\chi, \mathbf{u})\mathbf{T}^{-1} = \mathbf{R}(\chi, \mathbf{Tu}), \quad (13.2.2.2)$$

which is valid for any rotation  $\mathbf{T}$ , we obtain (see Appendix 13.2.1)

$$\mathbf{R}(\alpha, \beta, \gamma) = \mathbf{R}(\alpha, \mathbf{z})\mathbf{R}(\beta, \mathbf{y})\mathbf{R}(\gamma, \mathbf{z}). \quad (13.2.2.3)$$

The parameters  $(\alpha, \beta, \gamma)$  take values within the parallelepiped

$$0 \leq \alpha < 360; 0 \leq \beta \leq 180; 0 \leq \gamma < 360.$$

Here again, different values of the parameters may correspond to the same rotation, e.g.  $(\alpha, 180, \gamma)$  and  $(\alpha - \gamma, 180, 0)$ .

Although rotations are abstract objects, there is a one-to-one correspondence with the orthogonal matrices in three-dimensional space. In the following sections,  $\mathbf{R}$  will denote a  $3 \times 3$  orthogonal matrix. An explicit expression for the matrix which corresponds to the rotation  $(\chi, \mathbf{u})$  is

$$\begin{bmatrix} \cos \chi + u_1 u_1 (1 - \cos \chi) & u_1 u_2 (1 - \cos \chi) - u_3 \sin \chi & u_1 u_3 (1 - \cos \chi) + u_2 \sin \chi \\ u_2 u_1 (1 - \cos \chi) + u_3 \sin \chi & \cos \chi + u_2 u_2 (1 - \cos \chi) & u_2 u_3 (1 - \cos \chi) - u_1 \sin \chi \\ u_3 u_1 (1 - \cos \chi) - u_2 \sin \chi & u_3 u_2 (1 - \cos \chi) + u_1 \sin \chi & \cos \chi + u_3 u_3 (1 - \cos \chi) \end{bmatrix} \quad (13.2.2.4)$$

or, in condensed form,

$$\mathbf{R}(\chi, \mathbf{u})_{ij} = \delta_{ij} \cos \chi + u_i u_j (1 - \cos \chi) + \sum_{k=1}^3 \varepsilon_{ijk} u_k \sin \chi, \quad (13.2.2.5)$$

where  $\delta_{ij}$  is the Kronecker tensor,  $u_i$  are the components of  $\mathbf{u}$ , and  $\varepsilon_{ijk}$  is the Levi-Civita tensor. The rotation matrix in the Euler parameterization is obtained by substituting the matrices in the right-hand side of equation (13.2.2.3) by the corresponding expressions given by equation (13.2.2.4).

#### 13.2.2.1. The metric of the rotation group

The idea of distance between rotations is necessary for a correct formulation of the problem of sampling and for plotting functions of rotations (Burdina, 1971; Lattman, 1972). It can be demonstrated that the quantity

$$ds^2 = \text{Tr}(\mathbf{dR} \mathbf{dR}^+) = \sum_{i,j=1}^3 (\mathbf{dR}_{ij})^2 \quad (13.2.2.6)$$

defines a metric on the rotation group, unique up to a multiplicative

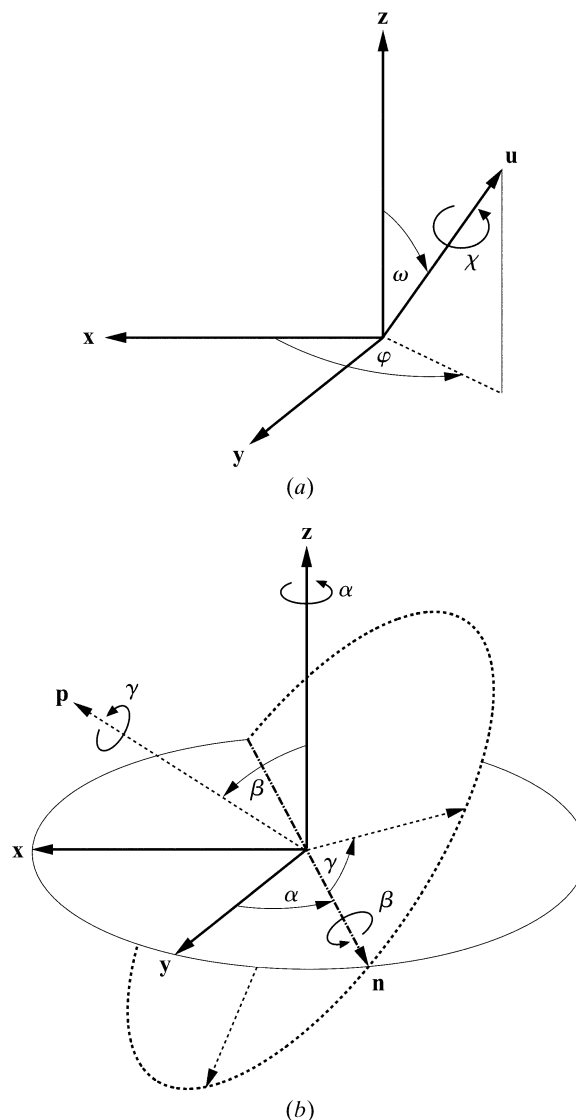


Fig. 13.2.2.1. Illustration of rotations defined by (a) the spherical polar angles  $(\chi, \omega, \varphi)$ ; (b) the Euler angles  $(\alpha, \beta, \gamma)$ .

### 13. MOLECULAR REPLACEMENT

constant, which cannot be reduced to a Cartesian metric. This is a topological property of the group, independent of its parameterization.  $ds$  is interpreted as the distance between the rotations  $\mathbf{R}$  and  $\mathbf{R} + d\mathbf{R}$ . With the Euler parameterization, equation (13.2.2.6) becomes

$$ds^2 = d\alpha^2 + 2 \cos(\beta) d\alpha d\gamma + d\gamma^2 + d\beta^2. \quad (13.2.2.7)$$

The volume element of integration,  $\sin(\beta) d\alpha d\beta d\gamma$ , corresponding to this length element guarantees the invariance of integrals over the rotation angles with respect to initial reference orientations.

The distance defined by equation (13.2.2.6) has a simple physical interpretation. Let us consider a molecule with initial atomic coordinates  $\{\mathbf{x}\}$ , referred to an orthonormal frame parallel to the molecule's principal moments of inertia,  $I_i$ . Then, the coordinates satisfy the conditions

$$\begin{aligned} \langle x_i x_j \rangle &= 0 \quad \text{if } i \neq j, \\ \langle x_i x_i \rangle &= I_i, \end{aligned} \quad (13.2.2.8)$$

where  $\langle \dots \rangle$  means 'average over atoms'. If we move the molecule from a rotated position characterized by the rotation  $\mathbf{R}$  to a close one characterized by  $\mathbf{R} + d\mathbf{R}$ , the mean-square shift of the atomic coordinates is

$$\sigma^2 = \langle (d\mathbf{R} \mathbf{x})^2 \rangle = \sum_{i=1}^3 I_i \sum_{j=1}^3 (dR_{ij})^2. \quad (13.2.2.9)$$

When all the  $I_i$  are equal,  $\sigma$  becomes proportional to  $ds$ .

#### 13.2.3. The rotation function

The absolute and relative orientations of the subunits that constitute a crystal may in principle be found by exploiting some properties of the Patterson function. We first express the crystal structure factors  $F(\mathbf{h})$  in terms of the Fourier transform of the electron density of isolated molecules,  $f_m(\mathbf{s})$ , calculated with their centres of gravity placed at the origin. If  $\mathbf{r}_m$  denotes the position within the crystal of the centre of gravity of the  $m$ th molecule, we have

$$F(\mathbf{h}) = \sum_{m=1}^M f_m(\mathbf{h}) \exp(2\pi i \mathbf{h} \mathbf{r}_m), \quad (13.2.3.1)$$

where  $M$  is the number of molecules within the unit cell. This is a general expression for  $F(\mathbf{h})$ , although the space-group and noncrystallographic rotational symmetries are not explicitly exhibited. The presence of symmetry implies that some of the  $f_m(\mathbf{h})$ 's are in fact samples of the same function at rotated arguments. The Fourier coefficients of the Patterson function can then be written as

$$\begin{aligned} I(\mathbf{h}) &= |F(\mathbf{h})|^2 = \sum_{m=1}^M |f_m(\mathbf{h})|^2 \\ &+ \sum_{m \neq m'=1}^M \overline{f_m(\mathbf{h})} f_{m'}(\mathbf{h}) \exp[2\pi i \mathbf{h} (\mathbf{r}_m - \mathbf{r}_{m'})], \end{aligned} \quad (13.2.3.2)$$

where  $\overline{f_m}$  is the complex conjugate of  $f_m$ . The first term in equation (13.2.3.2) involves only intramolecular contributions or self-Patterson terms; they are centred at the origin of the Patterson function. The second term involves intermolecular contributions or cross-Patterson terms; they are centred at the intermolecular vectors  $\mathbf{r}_m - \mathbf{r}_{m'}$ . Therefore, if we restrict the Patterson function to a region  $\Omega$ , of volume  $v$ , centred at the origin and having a dimension of the order of the dimensions of the isolated molecules, self-Patterson terms will dominate the crossed ones.

Thus it becomes possible to determine the rotation  $\mathbf{R}$  that superimposes one subunit upon an independent, homologous one by calculating the overlap within the region  $\Omega$  of the observed Patterson function (the target function  $P_t$ ) and a rotated version of either itself or the Patterson function of an isolated known molecule (the search function  $P_s$ ):

$$\mathcal{R}(\mathbf{R}) = (1/v) \int_{\Omega} P_t(\mathbf{r}) P_s(\mathbf{R}^{-1} \mathbf{r}) d^3 \mathbf{r} \quad (13.2.3.3)$$

(Rossmann & Blow, 1962).  $\mathcal{R}$  should display a local maximum for the sought rotation. Note that when we rotate the search function  $P_s$  by  $\mathbf{R}$ , its argument contains  $\mathbf{R}^{-1}$ . When the search and the target functions are the same,  $\mathcal{R}$  is called the self-rotation function; otherwise, it is called the cross-rotation function. When a model is available, the target data are calculated by placing the model within a  $P1$  cell whose dimensions guarantee that  $\Omega$  only contains self-Patterson contributions.

The reciprocal-space formulation of the above integral is obtained by substituting the Patterson functions by their Fourier summations:

$$P(\mathbf{r}) = \sum_{\mathbf{h}} [I(\mathbf{h})/V] \exp(-2\pi i \mathbf{h} \mathbf{r}). \quad (13.2.3.4)$$

Taking into account that  $I(-\mathbf{h}) = I(\mathbf{h})$ , we obtain

$$\begin{aligned} \mathcal{R}(\mathbf{R}) &= \sum_{\mathbf{h}} \sum_{\mathbf{k}} \frac{I_t(\mathbf{h}) I_s(\mathbf{k})}{V_t V_s} \frac{1}{v} \int_{\Omega} \exp[2\pi i (\mathbf{h} - \mathbf{k} \mathbf{R}^{-1}) \mathbf{r}] d^3 \mathbf{r} \\ &= \sum_{\mathbf{h}} \sum_{\mathbf{k}} \frac{I_t(\mathbf{h}) I_s(\mathbf{k})}{V_t V_s} \chi_{\Omega}(\mathbf{h} - \mathbf{k} \mathbf{R}^{-1}). \end{aligned} \quad (13.2.3.5)$$

$\chi_{\Omega}$ , the interference function, is the Fourier transform of the characteristic function of  $\Omega$ , *i.e.*, a function that takes the value 1 within  $\Omega$  and 0 outside. In principle, the domain of integration could have any shape. However, in order to take full advantage of the properties of the rotation group,  $\Omega$  is usually chosen as a spherical domain of radius  $b$ . Calling  $\mathbf{h} - \mathbf{k} \mathbf{R}^{-1} = \mathbf{s}$  for short, we have

$$\begin{aligned} \chi_b(\mathbf{s}) &= (3/4\pi b^3) \int_0^b \int_0^{\pi} \int_0^{2\pi} \exp(2\pi i \mathbf{s} \mathbf{r}) r^2 \sin(\theta) dr d\theta d\varphi \\ &= 3[\sin(2\pi s b) - 2\pi s b \cos(2\pi s b)] / (2\pi s b)^3. \end{aligned} \quad (13.2.3.6)$$

In the case of a spherical shell with inner and outer radii  $a$  and  $b$ , respectively, the interference function is obtained by subtraction:

$$[\chi_b(\mathbf{s}) - (a/b)^3 \chi_a(\mathbf{s})] / [1 - (a/b)^3]. \quad (13.2.3.7)$$

Although simple, the resulting expression for the rotation function has the disadvantage of containing entangled  $\mathbf{h}$ ,  $\mathbf{k}$  and  $\mathbf{R}$  contributions, which renders its computation time-consuming if the whole domain of rotations has to be explored. The difficulty may be overcome by expanding the exponentials entering equation (13.2.3.5) in spherical harmonics,  $Y_{\ell, m}$ . Taking advantage of their transformation under rotations, and using recurrence relationships between spherical Bessel functions,  $j_{\ell}$ , we obtain (see Appendix 13.2.1)

$$\begin{aligned} \chi_b(\mathbf{h} - \mathbf{k} \mathbf{R}^{-1}) &= \sum_{\ell=0}^{\infty} \sum_{m, m'=-\ell}^{\ell} \overline{Y_{\ell, m}(\hat{\mathbf{h}})} Y_{\ell, m'}(\hat{\mathbf{k}}) \\ &\times \left\{ \sum_{n=1}^{\infty} 12\pi [2(\ell + 2n) - 1] \frac{j_{\ell+2n-1}(2\pi h b)}{2\pi h b} \frac{j_{\ell+2n-1}(2\pi k b)}{2\pi k b} \right\} \\ &\times D_{m, m'}^{\ell}(\mathbf{R}), \end{aligned} \quad (13.2.3.8)$$

where  $D_{m, m'}^{\ell}$  are the matrices of the irreducible representations of the rotation group and  $\hat{\mathbf{h}}$  stands for 'angular part of vector  $\mathbf{h}$ '. The

## 13.2. ROTATION FUNCTIONS

awkwardness of equation (13.2.3.8) is apparent rather than real. Indeed:

(1) The expression separates angular from crystal variables. It also separates target from search contributions (see Section 13.2.3.1).

(2) The equation is accurate, even when truncating the summations on  $\ell$  and  $n$  to reasonable values (Navaza, 1993). The upper limit for  $\ell$  is of the order of the highest argument of the spherical Bessel functions,

$$\ell_{\max} \simeq 2\pi b/d_{\min},$$

where  $d_{\min}$  is the resolution of the data. The upper limit for  $n$  also depends on the current value of  $\ell$ ,

$$n_{\max}(\ell) \simeq (\ell_{\max} - \ell + 2)/2.$$

(3) When the rotations are parameterized in Euler angles ( $\alpha$ ,  $\beta$ ,  $\gamma$ ), the matrices  $D_{m, m'}^{\ell}$  take the form

$$D_{m, m'}^{\ell}(\alpha, \beta, \gamma) = d_{m, m'}^{\ell}(\beta) \exp[i(m\alpha + m'\gamma)], \quad (13.2.3.9)$$

which enables the computation of  $\mathcal{R}$ , for each given value of  $\beta$ , by means of two-dimensional fast Fourier transforms (FFTs).

This formulation is referred to as the fast rotation function (Crowther, 1972).

It may be useful to compare rotation functions obtained under different conditions. For this, some kind of normalization is needed. One possibility is to cast  $\mathcal{R}$  into the form of a correlation coefficient by dividing equation (13.2.3.3) by the norms of the truncated Patterson functions,

$$\mathcal{R}_N(\mathbf{R}) = \frac{\int_{\Omega} P_t(\mathbf{r}) P_s(\mathbf{R}^{-1}\mathbf{r}) d^3\mathbf{r}}{\left[ \int_{\Omega} P_t(\mathbf{r})^2 d^3\mathbf{r} \int_{\Omega} P_s(\mathbf{r})^2 d^3\mathbf{r} \right]^{1/2}}. \quad (13.2.3.10)$$

### 13.2.3.1. Computing the rotation function

A direct evaluation of equation (13.2.3.3) is possible. However, since the values of the Patterson functions are only available at discrete sampling points, an interpolation is needed after each rotation. This method is known as the direct-space formulation of the rotation function (Nordman, 1966; Steigemann, 1974).

In the reciprocal-space formulation [equations (13.2.3.5) and (13.2.3.6)], some precautions are to be taken in order to save computing time:

(1) Use only strong reflections in the summations.

(2) For each  $\mathbf{kR}^{-1}$ , limit the summation on  $\mathbf{h}$  to vectors satisfying the condition  $|\mathbf{h} - \mathbf{kR}^{-1}| \leq 1/2\pi b$ .

In both formulations, it is worth using a distance between rotations to sample  $\mathcal{R}$  efficiently, as explained in Section 13.2.3.2.

For the fast rotation function [equations (13.2.3.5) and (13.2.3.8)], the calculations are organized as follows (Dodson, 1985; Navaza, 1993):

(1) Given the search and the target diffraction data, compute

$$e_{\ell, m, n} = \{12\pi[2(\ell + 2n) - 1]\}^{1/2} \times \sum_{\mathbf{h}} [I(\mathbf{h})/V] Y_{\ell, m}(\hat{\mathbf{h}}) [j_{\ell+2n-1}(2\pi h b)] / 2\pi h b \quad (13.2.3.11)$$

and normalize [to compute equation (13.2.3.10)]:

$$e_{\ell, m, n} \rightarrow e_{\ell, m, n} / \left( \sum_{\ell=2}^{\ell_{\max}} \sum_{m=-\ell}^{\ell} \sum_{n=1}^{n_{\max}(\ell)} |e_{\ell, m, n}|^2 \right)^{1/2}. \quad (13.2.3.12)$$

Odd  $\ell$  terms disappear, because the Friedel-related reflections contribute with opposite signs:

$$I(-\mathbf{h}) Y_{\ell, m}(-\hat{\mathbf{h}}) = (-1)^{\ell} I(\mathbf{h}) Y_{\ell, m}(\hat{\mathbf{h}}).$$

Also, if the Patterson function has an  $n$ -fold rotation axis along  $\mathbf{z}$ , only the terms with  $m$  equal to a multiple of  $n$  survive.

(2) Given the  $e_{\ell, m, n}$ 's, perform the sums

$$C_{m, m'}^{\ell} = \sum_{n=1}^{n_{\max}(\ell)} e_{\ell, m, n}^{(t)} e_{\ell, m', n}^{(s)}. \quad (13.2.3.13)$$

(3) For each  $\beta$  value, calculate the reduced matrix elements and compute

$$S_{m, m'}(\beta) = \sum_{\ell=2}^{\ell_{\max}} C_{m, m'}^{\ell} d_{m, m'}^{\ell}(\beta). \quad (13.2.3.14)$$

Then evaluate the  $\beta$  section of  $\mathcal{R}$  by FFT:

$$\mathcal{R}(\alpha, \beta, \gamma) = \sum_{m, m'=-\ell_{\max}}^{\ell_{\max}} S_{m, m'}(\beta) \exp[i(m\alpha + m'\gamma)]. \quad (13.2.3.15)$$

The sampling in  $\alpha$  and  $\gamma$  here is dictated by the standard FFT requirements.

### 13.2.3.2. Plotting and sampling the rotation function

An odd feature of the rotation domain is that quite different values of the parameters may correspond to very close rotations. This causes the graphic representation of the rotation function to be distorted. For example, when the Euler angle  $\beta$  is small or close to 180, a peak plotted on a Cartesian grid in  $\alpha$  and  $\gamma$  is strongly elongated in one direction. By redefining the reference orientation, the same peak near the  $\beta = 90$  section will have a quite different – natural – shape.

This problem may be partially overcome by using the distance between rotations introduced in Section 13.2.2.1. Although the metric cannot be reduced to a Cartesian one in three dimensions, it is possible to do so for two-dimensional sections. Indeed, for fixed  $\beta$ , the transformation

$$\begin{aligned} \omega_+ &= \cos(\beta/2)(\alpha + \gamma) \\ \omega_- &= \sin(\beta/2)(\alpha - \gamma) \end{aligned} \quad (13.2.3.16)$$

reduces equation (13.2.2.7) to  $ds^2 = d\omega_+^2 + d\omega_-^2$ . Therefore, distortion-free  $\beta$  sections may be plotted in terms of the variables  $\omega_{\pm}$  (Burdina, 1971; Lattman, 1972). Accordingly, a correct sampling of  $\mathcal{R}$  should consist of points regularly spaced in these variables. The number of points with respect to that of a regular spacing in  $\alpha$ ,  $\beta$  and  $\gamma$  is approximately

$$\int \sin(\beta) d\alpha d\beta d\gamma / \int d\alpha d\beta d\gamma = 2/\pi \simeq 0.64.$$

Notice that for  $\beta$  equal to 0 or 180, the sections reduce to lines.

In the case of the self-rotation function, when the order of the NCS may be anticipated, it is worth working with equation (13.2.2.6) in the polar parameterization,

$$ds^2 = d\chi^2 + [2 \sin(\chi/2)]^2 du^2. \quad (13.2.3.17)$$

For constant  $\chi$ , we have the topology of the spherical surface. It is then natural to plot the function as a stereographic projection.

In the case of the cross-rotation function, *i.e.*, when the atomic distribution of the search model is known, we may use equation (13.2.2.9) instead of equation (13.2.2.6) to define the sampling. For this, we choose  $\sigma$  as the smallest root-mean-square shift in atomic coordinates that produces an appreciable change in the value of the cross-rotation function. An acceptable sampling set of  $\mathcal{R}$  should then satisfy the following conditions:

(1) For every point in the rotation domain, there is at least one sampling point at a distance less than  $\sigma$ .

(2) The number of sampling points is as small as possible.

## 13. MOLECULAR REPLACEMENT

### 13.2.3.3. Strategies

Since the first attempts to detect subunits within the crystal asymmetric unit, a great deal of experience has been gained and the results collected in several treatises on molecular replacement (Rossmann, 1972; Machin, 1985; Dodson *et al.*, 1992; Carter & Sweet, 1997).

The success of the rotation function relies in part on the choice of the domain of integration, *i.e.*, inner and outer radii of the spherical domain, and limits on data resolution. The outer radius is chosen so as to maximize the ratio between the number of intramolecular and intermolecular vectors. A typical value of this radius is 50–75% of the subunit's diameter for spherical molecules. The choice of the inner radius is less crucial, provided that the origin peaks are subtracted from the Patterson functions; it is often set to zero.

The resolution range of the selected diffraction data depends on whether we are computing self- or cross-rotation functions. For self rotations, data up to the highest available resolution may be used. For cross rotations, the high-resolution limit is dictated by the degree of similarity between the probe and the actual molecules that constitute the crystal. The low-resolution limit is usually chosen so as to skip the solvent contribution.

Another parameter of interest concerns the angular resolution, which is rather specific to the fast rotation function. Although it was derived by expanding the interference function to follow the original reciprocal-space formulation as closely as possible, it may also be obtained by expanding the Patterson functions in spherical harmonics and then performing the integration (Crowther, 1972). In this way, the concept of angular resolution is more evident. In fact, the spherical harmonics play the same role in the angular domain as the imaginary exponentials do in Cartesian coordinate space. The analogue of the Miller indexes here is the label  $\ell$ , directly related to the angular resolution. The term with  $\ell = 0$  is invariant under rotations and is thus eliminated from the summation in equation (13.2.3.14). It represents the contribution of the best radial functions, in a least-squares sense, that approximate the Patterson functions within  $\Omega$ . The origin peak is thus properly removed by omitting the  $\ell = 0$  term, as well as a substantial component of the original function. Also, by omitting low  $\ell$ 's, the angular resolution of peaks is enhanced. These eliminations may also be done in other formulations, but never as efficiently.

The parameters discussed above are not all independent. The relationship between them stems from the behaviour of the spherical Bessel functions for small values of their argument (Watson, 1958),

$$j_\ell(2\pi hb) \simeq (2\pi hb)^\ell / (2\ell + 1)!!$$

[see equation (13.2.3.8)]. So, when omitting low  $\ell$  terms, we are also weighting down low-resolution data.

### 13.2.3.4. Symmetry properties of the rotation function

The overlap integral that defines  $\mathcal{R}$  may be calculated by rotating  $P_t$  instead of  $P_s$ , but with the inverse rotation,

$$\begin{aligned} \mathcal{R}(\mathbf{R}) &= (1/v) \int_{\Omega} P_t(\mathbf{r}) P_s(\mathbf{R}^{-1}\mathbf{r}) d^3\mathbf{r} \\ &= (1/v) \int_{\Omega} P_t(\mathbf{R}\mathbf{r}) P_s(\mathbf{r}) d^3\mathbf{r}. \end{aligned} \quad (13.2.3.18)$$

This property enables the analysis of the consequence of the symmetries of the Patterson functions upon the rotation function (Tollin *et al.*, 1966; Moss, 1985). For example, when the target and search functions are the same, a trivial symmetry of the self-rotation results: its values at  $\mathbf{R}$  and  $\mathbf{R}^{-1}$  are the same or, in Euler angles, at  $(\alpha, \beta, \gamma)$  and  $(180 - \gamma, \beta, 180 - \alpha)$ . More generally, if  $P_t$  is invariant under the rotation  $\mathbf{T}$ , *i.e.*,  $P_t(\mathbf{T}^{-1}\mathbf{r}) = P_t(\mathbf{r})$  [and similarly

for the search function,  $P_s(\mathbf{S}^{-1}\mathbf{r}) = P_s(\mathbf{r})$ ], then

$$\begin{aligned} \mathcal{R}(\mathbf{R}) &= (1/v) \int_{\Omega} P_t(\mathbf{r}) P_s(\mathbf{R}^{-1}\mathbf{r}) d^3\mathbf{r} \\ &= (1/v) \int_{\Omega} P_t(\mathbf{T}^{-1}\mathbf{r}) P_s(\mathbf{S}^{-1}\mathbf{R}^{-1}\mathbf{r}) d^3\mathbf{r} \\ &= (1/v) \int_{\Omega} P_t(\mathbf{r}) P_s(\mathbf{S}^{-1}\mathbf{R}^{-1}\mathbf{T}\mathbf{r}) d^3\mathbf{r} = \mathcal{R}(\mathbf{T}^{-1}\mathbf{R}\mathbf{S}). \end{aligned} \quad (13.2.3.19)$$

However, the actual symmetry displayed by  $\mathcal{R}$  depends on the parameterization of the rotations and on the orientation of the orthonormal axes with respect to the crystal ones. Within the Euler parameterization, if the target function has an  $n$ -fold rotation axis parallel to the orthonormal  $z$  axis, then, according to equation (13.2.2.3),  $\mathcal{R}$  will have a periodicity of  $360/n$  along  $\alpha$ . Similarly, a rotation axis of order  $n$  along  $\mathbf{z}$  of  $P_s$  gives rise to a periodicity of  $360/n$  along  $\gamma$ . Therefore, the amount of calculation is reduced by choosing  $\mathbf{z}$  along the Patterson functions' highest rotational symmetry axes [see equation (13.2.3.11)].

### 13.2.4. The locked rotation function

The rotational NCS, determined with the help of the self-rotation function, may be used to enhance the signal-to-noise ratio of cross-rotation functions (Rossmann *et al.*, 1972; Tong & Rossmann, 1990). If  $\{\mathbf{S}_n, n = 1, \dots, N\}$  denotes the set of NCS rotations, including the identity, and  $\mathbf{R}$  is a correct orientation of the cross rotation, then  $\mathbf{S}_n\mathbf{R}$  must also correspond to a correct orientation. Here we are assuming that the rotational NCS forms a group. Otherwise, either  $\mathbf{S}_n\mathbf{R}$  or  $\mathbf{S}_n^{-1}\mathbf{R}$ , but not both, corresponds to another correct orientation. Therefore, a function may be defined, the locked cross rotation, whose values are the average of the cross-rotation values at orientations related by the NCS:

$$\mathcal{R}_{LC}(\mathbf{R}) = \sum_{n=1}^N \mathcal{R}(\mathbf{S}_n\mathbf{R}) / N. \quad (13.2.4.1)$$

By redefining the target function, it can be computed as an ordinary cross rotation. Indeed,  $\mathcal{R}_{LC}$  may be written in a form similar to equation (13.2.3.3),

$$\begin{aligned} \mathcal{R}_{LC}(\mathbf{R}) &= \sum_{n=1}^N (1/v) \int_{\Omega} P_t(\mathbf{r}) P_s(\mathbf{R}^{-1}\mathbf{S}_n^{-1}\mathbf{r}) d^3\mathbf{r} / N \\ &= (1/v) \int_{\Omega} \left[ \sum_{n=1}^N P_t(\mathbf{S}_n\mathbf{r}) / N \right] P_s(\mathbf{R}^{-1}\mathbf{r}) d^3\mathbf{r}, \end{aligned} \quad (13.2.4.2)$$

with the target Patterson function substituted by the average over the NCS of the rotated target functions. The computation of equation (13.2.4.2) is particularly simple in the case of the fast rotation function. The substitution

$$e_{\ell, m, n}^{(t)} \rightarrow \sum_{m'=-\ell}^{\ell} \left[ \sum_{n=1}^N \mathcal{D}_{m, m'}^{\ell}(\mathbf{S}_n) / N \right] e_{\ell, m', n}^{(t)}, \quad (13.2.4.3)$$

where we replaced the sum over  $\mathbf{S}_n^{-1}$  by a sum over  $\mathbf{S}_n$ , because of the rearrangement theorem of group theory, gives the required target coefficients.

The same ideas may be applied to the self-rotation function. Here the NCS is assumed beforehand, with elements  $\{\mathbf{I}_n, n = 1, \dots, N\}$  in a given reference orientation. They are related to the actual NCS elements by

$$\mathbf{S}_n = \mathbf{R}_n \mathbf{I}_n \mathbf{R}_n^{-1} \quad (13.2.4.4)$$

[see equation (13.2.2.2)]. Since each  $\mathbf{S}_n$  should correspond to a local

maximum of the self rotation, the function

$$\mathcal{R}_{LS}(\mathbf{R}) = \sum_{n=1}^N \mathcal{R}(\mathbf{R}\mathbf{I}_n\mathbf{R}^{-1})/N \quad (13.2.4.5)$$

should also display a maximum for each  $\mathbf{R}_n$ , but with a noise level reduced by  $(N)^{1/2}$ . Equation (13.2.4.5) defines the locked self-rotation function. Its computation by fast rotation techniques is less straightforward than in the locked cross-rotation case.

### 13.2.5. Other rotation functions

The rotation function was hitherto described in terms of self- and cross-Patterson vectors. This is perhaps inevitable in the self-rotation case, but the problem of determining the absolute orientation of the subunits when a model structure is available may be formulated in a different way. We may try to compare directly the observed and calculated intensities or structure factors by using any criterion analogous to those employed in refinement procedures, *e.g.*, the crystallographic  $R$  factor or correlation coefficients.

When the space-group symmetry is explicitly exhibited, the structure factor corresponding to a crystal with  $M$  independent molecules in the unit cell takes the form

$$F(\mathbf{h}) = \sum_{m=1}^M \sum_{g=1}^G f_m(\mathbf{h}\mathbf{M}_g) \exp[2\pi i\mathbf{h}(\mathbf{M}_g\mathbf{r}_m + \mathbf{t}_g)], \quad (13.2.5.1)$$

where  $\mathbf{M}_g$  and  $\mathbf{t}_g$  denote, respectively, the transformation matrix and the translation associated with the  $g$ th symmetry operation of the crystal space group. The corresponding intensity is

$$I(\mathbf{h}) = \sum_{m,m'=1}^M \sum_{g,g'=1}^G \overline{f_m(\mathbf{h}\mathbf{M}_g)} f_{m'}(\mathbf{h}\mathbf{M}_{g'}) \times \exp[2\pi i\mathbf{h}(\mathbf{M}_g\mathbf{r}_m + \mathbf{t}_g - \mathbf{M}_{g'}\mathbf{r}_{m'} - \mathbf{t}_{g'})]. \quad (13.2.5.2)$$

For criteria based on amplitudes, the calculated structure factor will contain only the contribution of the rotated model,

$$F_{\mathbf{h}}^{\text{calc}}(\mathbf{R}) = f_m(\mathbf{h}\mathbf{R}), \quad (13.2.5.3)$$

*i.e.*, the Fourier transform of a single molecule in the crystal cell, assuming  $P1$  symmetry. For criteria based on intensities, some symmetry information may be introduced,

$$I_{\mathbf{h}}^{\text{calc}}(\mathbf{R}) = \sum_{g=1}^G |f_m(\mathbf{h}\mathbf{M}_g\mathbf{R})|^2. \quad (13.2.5.4)$$

A criterion often considered is the correlation coefficient on intensities,

$$\mathcal{R}_{\mathcal{D}}(\mathbf{R}) = \langle (I^{\text{obs}} - \langle I^{\text{obs}} \rangle)(I^{\text{calc}} - \langle I^{\text{calc}} \rangle) \rangle \times [ \langle (I^{\text{obs}} - \langle I^{\text{obs}} \rangle)^2 \rangle \langle (I^{\text{calc}} - \langle I^{\text{calc}} \rangle)^2 \rangle ]^{1/2}, \quad (13.2.5.5)$$

where  $\langle \dots \rangle$  means 'average over reflections'. It may be calculated within reasonable computing time provided that

- (1) the structure factors are computed by interpolation from the Fourier transform of the isolated molecule's electron density; and
- (2) an efficient sampling set of  $\mathcal{R}_{\mathcal{D}}$  is defined.

$\mathcal{R}_{\mathcal{D}}$  is referred to as the direct-rotation function (DeLano & Brünger, 1995). A major advantage of this formulation is that the information stemming from already-positioned subunits may be taken into account, just by adding their contribution to the calculated intensities.

### 13.2.6. Concluding remarks

Each formulation of the rotation function described above has its advantages and disadvantages. The direct-space formulation [equation (13.2.3.3)] offers the possibility of modifying the Patterson function or selecting the strongest peaks to be used in the overlap integral. Also, the domain of integration may have any shape, as in the reciprocal-space formulation [equation (13.2.3.5)]. However, in both formulations, the numerical results can be somewhat imprecise because of the approximations introduced to save computing time.

When the domain of integration is spherical, as is usually the case, then the fast rotation function [equation (13.2.3.15)] is faster, more accurate and allows for angular-resolution enhancement. Moreover, since most of the computing time is spent in the calculation of the coefficients  $e_{\ell,m,n}$ , a library of these coefficients may be compiled to assess the models in a given molecular-replacement problem more rapidly.

The direct rotation [equation (13.2.5.5)] seems preferable to the cross-rotation function, as it includes all self-Patterson terms of the search model. However, when the order of the space group is high, the calculated intensity represents only a small fraction of the observed one, and the discriminative power of the function drops, as compared with the cross-rotation function.

Patterson searches now benefit from new supercomputers. The real problem of molecular replacement, split for convenience into rotation and translation searches, is beginning to be tackled by genuine six-dimensional searches where all orientations are tested. This may represent the end of cross-rotation and direct-rotation functions.

### Appendix 13.2.1.

#### Formulae for the derivation and computation of the fast rotation function

This appendix aims to present a complete set of formulae which allow the derivation and computation of the fast rotation function. They involve a particular convention for the definition of the irreducible representations of the rotation group suitable for crystallographic computations.

##### A13.2.1.1. Euler parameterization

By applying the group property of rotations [equation (13.2.2.2)], the Euler parameterization may be expressed as rotations around fixed axis (see Fig. 13.2.2.1b):

$$\begin{aligned} \mathbf{R}(\alpha, \beta, \gamma) &= \mathbf{R}(\gamma, \mathbf{p})\mathbf{R}(\beta, \mathbf{n})\mathbf{R}(\alpha, \mathbf{z}) \\ &= \left[ \mathbf{R}(\beta, \mathbf{n})\mathbf{R}(\gamma, \mathbf{z})\mathbf{R}(\beta, \mathbf{n})^{-1} \right] \mathbf{R}(\beta, \mathbf{n})\mathbf{R}(\alpha, \mathbf{z}) \\ &= \mathbf{R}(\beta, \mathbf{n})\mathbf{R}(\gamma, \mathbf{z})\mathbf{R}(\alpha, \mathbf{z}) \\ &= \left[ \mathbf{R}(\alpha, \mathbf{z})\mathbf{R}(\beta, \mathbf{y})\mathbf{R}(\alpha, \mathbf{z})^{-1} \right] \mathbf{R}(\gamma, \mathbf{z})\mathbf{R}(\alpha, \mathbf{z}) \\ &= \mathbf{R}(\alpha, \mathbf{z})\mathbf{R}(\beta, \mathbf{y})\mathbf{R}(\gamma, \mathbf{z}). \end{aligned} \quad (\text{A13.2.1.1})$$

##### A13.2.1.2. The $D_{m,m'}^{\ell}$ matrices

A linear representation of dimension  $n$  of the rotation group is a correspondence between rotations and matrices of order  $n$ . The matrices  $D_{m,m'}^{\ell}(\mathbf{R})$ , with  $-\ell \leq m, m' \leq \ell$ , are associated with the irreducible representation of dimension  $2\ell + 1$  ( $0 \leq \ell < \infty$ ). They have the following properties (Brink & Satchler, 1968):

### 13. MOLECULAR REPLACEMENT

(1) Group multiplication:

$$D_{m, m'}^{\ell}(\mathbf{R}\mathbf{R}') = \sum_{n=-\ell}^{\ell} D_{m, n}^{\ell}(\mathbf{R})D_{n, m'}^{\ell}(\mathbf{R}'). \quad (\text{A13.2.1.2})$$

(2) Complex conjugation:

$$D_{m, m'}^{\ell}(\mathbf{R}^{-1}) = \overline{D_{m', m}^{\ell}(\mathbf{R})}. \quad (\text{A13.2.1.3})$$

(3) Euler parameterization:

$$D_{m, m'}^{\ell}(\alpha, \beta, \gamma) = d_{m, m'}^{\ell}(\beta) \exp[i(m\alpha + m'\gamma)]. \quad (\text{A13.2.1.4})$$

(4) Recurrence relation for the reduced matrices:

$$d_{m-1, m'}^{\ell}(\beta) = \frac{[m' - m \cos(\beta)]^2}{[(\ell - m + 1)(\ell + m)]^{1/2} \sin(\beta)} d_{m, m'}^{\ell}(\beta) - \left[ \frac{(\ell - m)(\ell + m + 1)}{(\ell - m + 1)(\ell + m)} \right]^{1/2} d_{m+1, m'}^{\ell}(\beta). \quad (\text{A13.2.1.5})$$

(5) Initial values (bottom row of  $d^{\ell}$ ):

$$d_{\ell, m}^{\ell}(\beta) = (-1)^{\ell-m} \left[ \frac{(2\ell)!}{(\ell - m)!(\ell + m)!} \right]^{1/2} \sin(\beta/2)^{\ell-m} \cos(\beta/2)^{\ell+m}. \quad (\text{A13.2.1.6})$$

(6) Symmetry relations:

$$d_{-m, -m'}^{\ell}(\beta) = d_{m', m}^{\ell}(\beta) = (-1)^{m-m'} d_{m, m'}^{\ell}(\beta). \quad (\text{A13.2.1.7})$$

#### A13.2.1.3. Spherical harmonics

The  $Y_{\ell, m}$ 's, with  $-\ell \leq m \leq \ell$  and  $0 \leq \ell < \infty$ , constitute a complete set of functions of the unit vector  $\mathbf{u}$ , having the following properties (Brink & Satchler, 1968):

(1) Transformation under rotations:

$$Y_{\ell, m}(\mathbf{R}^{-1}\mathbf{u}) = \sum_{m'=-\ell}^{\ell} D_{m, m'}^{\ell}(\mathbf{R}^{-1})Y_{\ell, m'}(\mathbf{u}) = \sum_{m'=-\ell}^{\ell} Y_{\ell, m'}(\mathbf{u})\overline{D_{m', m}^{\ell}(\mathbf{R})}. \quad (\text{A13.2.1.8})$$

(2) Orthogonality condition:

$$\int \overline{Y_{\ell, m}(\mathbf{u})} Y_{\ell', m'}(\mathbf{u}) d^2\mathbf{u} = \delta_{\ell, \ell'} \delta_{m, m'}. \quad (\text{A13.2.1.9})$$

(3) Inversion:

$$Y_{\ell, m}(-\mathbf{u}) = (-1)^{\ell} Y_{\ell, m}(\mathbf{u}). \quad (\text{A13.2.1.10})$$

(4) Relation with rotation-matrix elements:

$$Y_{\ell, m}(\theta, \varphi) = i^{\ell} [(2\ell + 1)/4\pi]^{1/2} D_{m, 0}^{\ell}(\varphi, \theta, 0), \quad (\text{A13.2.1.11})$$

where  $(\theta, \varphi)$  are the polar coordinates of  $\mathbf{u}$ .

#### A13.2.1.4. Spherical Bessel functions

The  $j_{\ell}$ 's, with  $0 \leq \ell < \infty$ , constitute a complete set of functions having the following properties (Watson, 1958):

(1) Recurrence relation:

$$j_{\ell-1}(x) - (2\ell + 1)[j_{\ell}(x)/x] + j_{\ell+1}(x) = 0. \quad (\text{A13.2.1.12})$$

(2) Initial values:

$$j_0(x) = \sin(x)/x \\ j_1(x) = [\sin(x) - x \cos(x)]/x^2. \quad (\text{A13.2.1.13})$$

(3) Integral of a product of spherical Bessel functions:

$$U^{\ell}(p, q) = \int_0^1 j_{\ell}(px)j_{\ell}(qx)x^2 dx \\ = \begin{cases} [j_{\ell}(p)j_{\ell-1}(q)q - j_{\ell}(q)j_{\ell-1}(p)p]/(p^2 - q^2) & \text{if } p \neq q \\ \frac{1}{2}[j_{\ell}(p)^2 - j_{\ell-1}(p)j_{\ell+1}(p)] & \text{if } p = q \end{cases} \\ = (2\ell + 3)[j_{\ell+1}(p)j_{\ell+1}(q)]/pq + U^{\ell+2}(p, q) \\ = \sum_{n=1}^{\infty} [2(\ell + 2n) - 1][j_{\ell+2n-1}(p)j_{\ell+2n-1}(q)]/pq. \quad (\text{A13.2.1.14})$$

#### A13.2.1.5. Expansion of $\exp(2\pi i \mathbf{s} \cdot \mathbf{r})$

This is also called the plane-wave expansion or Laplace's expansion (Landau & Lifschitz, 1972):

$$\exp(2\pi i \mathbf{s} \cdot \mathbf{r}) = 4\pi \sum_{\ell=0}^{\infty} i^{\ell} \sum_{m=-\ell}^{\ell} j_{\ell}(2\pi s r) \overline{Y_{\ell, m}(\hat{\mathbf{s}})} Y_{\ell, m}(\hat{\mathbf{r}}). \quad (\text{A13.2.1.15})$$

#### A13.2.1.6. Expansion of the interference function

$$\chi_b(\mathbf{h} - \mathbf{h}\mathbf{R}^{-1}) = (3/4\pi b^3) \int_0^b \int_0^{\pi} \int_0^{2\pi} \exp[2\pi i(\mathbf{h} - \mathbf{h}\mathbf{R}^{-1})\mathbf{r}] r^2 \sin(\theta) dr d\theta d\varphi \\ = \sum_{\ell, \ell'=0}^{\infty} \sum_{m=-\ell}^{\ell} \sum_{m'=-\ell'}^{\ell'} i^{\ell-\ell'} \overline{Y_{\ell, m}(\hat{\mathbf{h}})} Y_{\ell', m'}(\hat{\mathbf{k}}) \\ \times (12\pi/b^3) \int_0^b j_{\ell}(2\pi hr) j_{\ell'}(2\pi kr) r^2 dr \\ \times \int_0^{\pi} \int_0^{2\pi} Y_{\ell, m}(\hat{\mathbf{r}}) \overline{Y_{\ell', m'}(\mathbf{R}^{-1}\hat{\mathbf{r}})} \sin(\theta) d\theta d\varphi \\ = \sum_{\ell=0}^{\infty} \sum_{m=-\ell}^{\ell} \sum_{\ell'=0}^{\infty} \sum_{m'=-\ell'}^{\ell'} i^{\ell-\ell'} \overline{Y_{\ell, m}(\hat{\mathbf{h}})} Y_{\ell', m'}(\hat{\mathbf{k}}) \\ \times (12\pi/b^3) \int_0^b j_{\ell}(2\pi hr) j_{\ell'}(2\pi kr) r^2 dr \\ \times \sum_{m''=-\ell' 0}^{\ell'} \int_0^{\pi} \int_0^{2\pi} Y_{\ell, m}(\hat{\mathbf{r}}) \overline{Y_{\ell', m''}(\hat{\mathbf{r}})} \sin(\theta) d\theta d\varphi D_{m'', m'}^{\ell'}(\mathbf{R}) \\ = \sum_{\ell=0}^{\infty} \sum_{m'=-\ell}^{\ell} \overline{Y_{\ell, m}(\hat{\mathbf{h}})} Y_{\ell, m'}(\hat{\mathbf{k}}) 12\pi U^{\ell}(2\pi hb, 2\pi kb) D_{m, m'}^{\ell}(\mathbf{R}). \quad (\text{A13.2.1.16})$$

## REFERENCES

## 13.1 (cont.)

- Jack, A. (1973). *Direct determination of X-ray phases for tobacco mosaic virus protein using non-crystallographic symmetry*. *Acta Cryst.* **A29**, 545–554.
- Kayushina, R. L. & Vainshtein, B. K. (1965). *Rentgenografiye opredelenie strukturi L-prolina*. *Kristallografiya*, **10**, 833–844.
- Kissinger, C. R., Gehlhaar, D. K. & Fogel, D. B. (1999). *Rapid automated molecular replacement by evolutionary search*. *Acta Cryst.* **D55**, 484–491.
- Lattman, E. E. & Love, W. E. (1970). *A rotational search procedure for detecting a known molecule in a crystal*. *Acta Cryst.* **B26**, 1854–1857.
- Lawrence, M. C. (1991). *The application of the molecular replacement method to the de novo determination of protein structure*. *Q. Rev. Biophys.* **24**, 399–424.
- McKenna, R., Xia, D., Willingmann, P., Ilag, L. L. & Rossmann, M. G. (1992). *Structure determination of the bacteriophage  $\phi$ X174*. *Acta Cryst.* **B48**, 499–511.
- Matthews, B. W., Sigler, P. B., Henderson, R. & Blow, D. M. (1967). *Three-dimensional structure of tosyl- $\alpha$ -chymotrypsin*. *Nature (London)*, **214**, 652–656.
- Milledge, H. J. (1962). *The automatic selection of molecular-crystal structure by combining stereochemical criteria and high-speed computing*. *Proc. R. Soc. London Ser. A*, **267**, 566–589.
- Nordman, C. E. & Nakatsu, K. (1963). *Interpretation of the Patterson function of crystals containing a known molecular fragment. The structure of an Alstonia alkaloid*. *J. Am. Chem. Soc.* **85**, 353.
- Prothero, J. W. & Rossmann, M. G. (1964). *The relative orientation of molecules of crystallized human and horse oxyhaemoglobin*. *Acta Cryst.* **17**, 768–769.
- Rossmann, M. G. (1990). *The molecular replacement method*. *Acta Cryst.* **A46**, 73–82.
- Rossmann, M. G. (1995). *Ab initio phase determination and phase extension using non-crystallographic symmetry*. *Curr. Opin. Struct. Biol.* **5**, 650–655.
- Rossmann, M. G. & Arnold, E. (2001). *Patterson and molecular-replacement techniques*. In *International tables for crystallography*, Vol. B. *Reciprocal space*, edited by U. Shmueli, pp. 235–263. Dordrecht: Kluwer Academic Publishers.
- Rossmann, M. G. & Blow, D. M. (1962). *The detection of sub-units within the crystallographic asymmetric unit*. *Acta Cryst.* **15**, 24–31.
- Rossmann, M. G. & Blow, D. M. (1963). *Determination of phases by the conditions of non-crystallographic symmetry*. *Acta Cryst.* **16**, 39–45.
- Rossmann, M. G., Blow, D. M., Harding, M. M. & Collier, E. (1964). *The relative positions of independent molecules within the same asymmetric unit*. *Acta Cryst.* **17**, 338–342.
- Rossmann, M. G., McKenna, R., Tong, L., Xia, D., Dai, J.-B., Wu, H., Choi, H.-K. & Lynch, R. E. (1992). *Molecular replacement real-space averaging*. *J. Appl. Cryst.* **25**, 166–180.
- Schevitz, R. W., Podjarny, A. D., Zwick, M., Hughes, J. J. & Sigler, P. B. (1981). *Improving and extending the phases of medium- and low-resolution macromolecular structure factors by density modification*. *Acta Cryst.* **A37**, 669–677.
- Scouloudi, H. (1969). *X-ray crystallographic studies of seal myoglobin at 6-Å and 5-Å resolution*. *J. Mol. Biol.* **40**, 353–377.
- Sheriff, S., Klei, H. E. & Davis, M. E. (1999). *Implementation of a six-dimensional search using the AMoRe translation function for difficult molecular-replacement problems*. *J. Appl. Cryst.* **32**, 98–101.
- Tollin, P. (1969). *Determination of the orientation and position of the myoglobin molecule in the crystal of seal myoglobin*. *J. Mol. Biol.* **45**, 481–490.
- Tollin, P. & Cochran, W. (1964). *Patterson function interpretation for molecules containing planar groups*. *Acta Cryst.* **17**, 1322–1324.
- Wang, B. C. (1985). *Resolution of phase ambiguity in macromolecular crystallography*. *Methods Enzymol.* **115**, 90–92.
- Wilson, I. A., Skehel, J. J. & Wiley, D. C. (1981). *Structure of the haemagglutinin membrane glycoprotein of influenza virus at 3 Å resolution*. *Nature (London)*, **289**, 366–373.

## 13.2

- Brink, D. M. & Satchler, G. R. (1968). *Angular momentum*, 2nd ed. Oxford University Press.
- Burdina, V. I. (1971). *Symmetry of rotation function*. *Sov. Phys. Crystallogr.* **15**, 545–550.
- Carter, C. W. & Sweet, R. M. (1997). *Molecular replacement*. *Methods Enzymol.* **276**, 558–619.
- Crowther, R. A. (1972). In *The molecular replacement method*, edited by M. G. Rossmann, pp. 173–178. New York: Gordon and Breach.
- DeLano, W. L. & Brünger, A. T. (1995). *The direct rotation function: rotational Patterson correlation search applied to molecular replacement*. *Acta Cryst.* **D51**, 740–748.
- Dodson, E. J. (1985). In *Proceedings of the Daresbury study weekend. Molecular replacement*, edited by P. A. Machin, pp. 33–45. Warrington: Daresbury Laboratory.
- Dodson, E. J., Gover, S. & Wolf, W. (1992). Editors. *Proceedings of the Daresbury study weekend. Molecular replacement*. Warrington: Daresbury Laboratory.
- Landau, L. D. & Lifschitz, E. M. (1972). *Théorie quantique relativiste*, pp. 109–196. Moscow: Editions MIR.
- Lattman, E. E. (1972). *Optimal sampling of the rotation function*. *Acta Cryst.* **B28**, 1065–1068.
- Machin, P. A. (1985). Editor. *Proceedings of the Daresbury study weekend. Molecular replacement*. Warrington: Daresbury Laboratory.
- Moss, D. S. (1985). *The symmetry of the rotation function*. *Acta Cryst.* **A41**, 470–475.
- Navaza, J. (1993). *On the computation of the fast rotation function*. *Acta Cryst.* **D49**, 588–591.
- Nordman, C. E. (1966). *Vector space search and refinement procedures*. *Trans. Am. Crystallogr. Assoc.* **2**, 29–38.
- Rossmann, M. G. (1972). Editor. *The molecular replacement method*. New York: Gordon and Breach.
- Rossmann, M. G. & Blow, D. M. (1962). *The detection of sub-units within the crystallographic asymmetric unit*. *Acta Cryst.* **15**, 24–31.
- Rossmann, M. G., Ford, G. C., Watson, H. C. & Banaszak, L. J. (1972). *Molecular symmetry of glyceraldehyde-3-phosphate dehydrogenase*. *J. Mol. Biol.* **64**, 237–245.
- Steigemann, W. (1974). *Die Entwicklung und Anwendung von Rechenverfahren und Regenprogrammen zur Strukturanalyse von Proteinen am Beispiel des Trypsin-Trypsin-inhibitor Komplexes, des Freien und der L-Asparaginase*. PhD thesis, Technische Universität, Munich, Germany.
- Tollin, P., Main, P. & Rossmann, M. G. (1966). *The symmetry of the rotation function*. *Acta Cryst.* **20**, 404–417.
- Tong, L. & Rossmann, M. G. (1990). *The locked rotation function*. *Acta Cryst.* **A46**, 783–792.
- Watson, G. N. (1958). *A treatise on the theory of Bessel functions*, 2nd ed. Cambridge University Press.

## 13.3

- Bentley, G. A. & Houdusse, A. (1992). *Some applications of the phased translation function in macromolecular structure determination*. *Acta Cryst.* **A48**, 312–322.
- Blow, D. M., Rossmann, M. G. & Jeffery, B. A. (1964). *The arrangement of  $\alpha$ -chymotrypsin molecules in the monoclinic crystal form*. *J. Mol. Biol.* **8**, 65–78.
- Brünger, A. T. (1990). *Extension of molecular replacement: a new search strategy based on Patterson correlation refinement*. *Acta Cryst.* **A46**, 46–57.